Available online at www.sciencedirect.com

SciVerse ScienceDirect

Ceramics International 39 (2013) 3987–3992

CERAMICS INTERNATIONAL

www.elsevier.com/locate/ceramint

Preparation of YAG nano-powders via an ultrasonic spray co-precipitation method

Yuliu You, Longhao Qi*, Xiaolei Li, Wei Pan

Department of Materials Science and Engineering, Tsinghua University, Beijing 100084, China

Received 30 June 2012; received in revised form 16 October 2012; accepted 25 October 2012
Available online 8 November 2012

Abstract

Nanometer-sized particles (1–100 nm) are of considerable interest for a wide variety of applications, due to their unique and improved properties primarily determined by size. In this study, homogenously dispersed nanocrystalline YAG powders were synthesized by calcination of the YAG precursors prepared by an ultrasonic spray method. The effects of spray droplets moving path, calcination temperature and aluminum ion concentration on the preparation of pure-phase YAG powders were intensively studied. The results show that the well-dispersed YAG nano-powders can be prepared by this ultrasonic spray co-precipitation method. Well-crystallized YAG powers can be generated when the precursors, produced through top symmetric spray with ammonia as precipitation agent, are calcined at 1000 °C for 3 h. The average size of YAG particles is about 50 nm and well-dispersed.

Keywords: Ultrasonic spray; Co-precipitation; YAG; Nano-powders

1. Introduction

Nd:YAG single crystal is one of the most important materials for solid-state laser application [1]. However the synthesis methods of Nd:YAG single crystal have many drawbacks such as low growth rate, expensive equipment and the limited doping concentration. Core at the central region of the single-crystal ingot and facets that exist from the central region to the outer region induce the limitation to the utilization of single crystals. For laser media, only the outer volume of the ingot is suitable, and thus the size of the laser medium is limited by the ingot size. Nd:YAG single crystals are grown at approximately 2000 °C, and the growth period is 1000–2000 h. Because the Nd segregation coefficient for YAG is 0.2 and solubility during growth of Nd in YAG is ~1 at%, the light absorption coefficient of commercial single crystals is low, and such crystals present a drawback of concentration quenching. Recently, tremendous efforts have been taken to develop the alternatives for Nd:YAG single crystal. Compared with Nd:YAG single crystal, polycrystalline Nd:YAG ceramics has many advantages, such as the simple synthesis process, low cost, high concentration doping and better homogeneity of doping ions [2]. As is known to all, it is difficult to prepare transparent ceramics with conventional materials and conventional methods [3]. Synthesis of high quality nano-powders is the first and key step for preparation of highly transparent ceramics [4].

YAG powders were usually prepared by the solid-state reaction method for its low cost and simple process [5–11]. Recent studies showed, however, YAG powders prepared with chemical methods was preferable for sintering transparent ceramics compared with powders from the solid-state reaction method, for solution-based techniques can achieve better chemical homogeneity [12]. Consequently, several liquid-chemical synthesis methods have been developed, such as co-precipitation [13–22], homogeneous precipitation [23–26], sol–gel processing [27–31], hydrothermal treatment [32], spray pyrolysis [33], etc.

In this paper, YAG precursors were first co-precipitated by using the ultrasonic spray method. The effect of spray droplets moving path, calcination temperature and aluminum ion concentration on the preparation of pure-phase YAG

*Corresponding author. Tel.: +86 13901071643.
E-mail address: qilonghao@yahoo.cn (L. Qi).

0272-8842/$ - see front matter © 2012 Elsevier Ltd and Techna Group S.r.l. All rights reserved.
http://dx.doi.org/10.1016/j.ceramint.2012.10.248

powders have been mainly studied. The method is based on ultrasonic generation of micro-sized droplets. Each micro-droplet can be considered as a "microreactor", so there is no need to manufacture a real, physical microreactor for the reaction, and thus the cost will be greatly reduced and the process can be extensively simplified.

What is more, microdroplets would also avoid the heterogeneous local concentration in the liquid system and uneven nucleation which are the two main reasons for poor stoichiometry and nonuniform particle size.

2. Experiment

Yttrium nitrate hexahydrate ($Y(NO_3)_3 \cdot 6H_2O$, AR, Sinopharm Chemical Reagent Co., Ltd), aluminum nitrate hydrate ($Al(NO_3)_3 \cdot 9H_2O$, AR, Xiya Reagent Co., Ltd), and ammonia were used as raw materials. $Y(NO_3)_3 \cdot 6H_2O$ and $Al(NO_3)_3 \cdot 9H_2O$ in the molar ratio of 3:5 were dissolved into the deionized water to obtain a mixed solution in which the concentration of Al^{3+} was 0.5 mol/L or 1.0 mol/L. Ammonia was used as the precipitation agent. PEG (AR, Tianjin Guangfu Fine Chemical Reagent Research Institute) with 1 wt% of the mixed solution was added to prevent agglomeration.

Two devices were designed for the experiment. In both devices, ammonia as the precipitation agent was introduced through an entrance near the bottom. In device 1 (Fig. 1), ultrasonic nozzle was set on the side of the reactor while in device 2 (Fig. 2), the nozzle was set on the top. Therefore, the routes where the mixed solution was sprayed into the reactor are different. The products were collected in the deionized water which was put into the container beforehand. The ultrasonic vibrating frequency was 2.1×10^6 Hz. The precursors prepared by different processes were numbered in Table 1.

After ripening for 24 h, the precipitate precursors were washed with deionized water repeatedly and then with alcohol. The precursors were dried at 100 °C for 24 h and then calcined in air at different temperatures ranging from 800 °C to 1000 °C for 3 h with a heating rate of 5 °C/min.

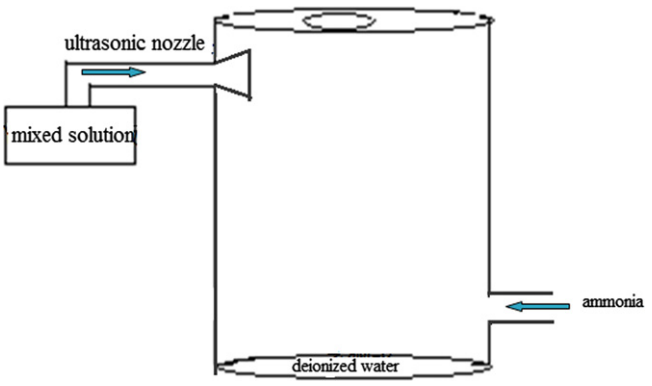

Fig. 1. Device 1.

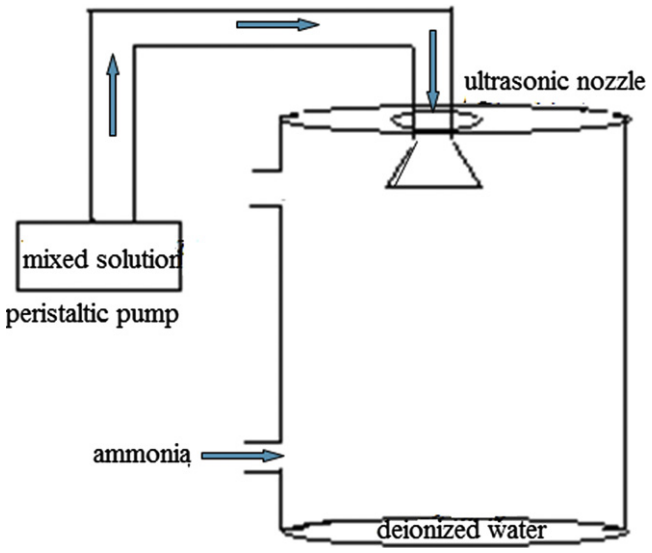

Fig. 2. Device 2.

Table1
Precursor number.

Precursor number	Concentration of Al^{3+} (mol/L)	Device number
①	0.5	1
②	1	1
③	0.5	2

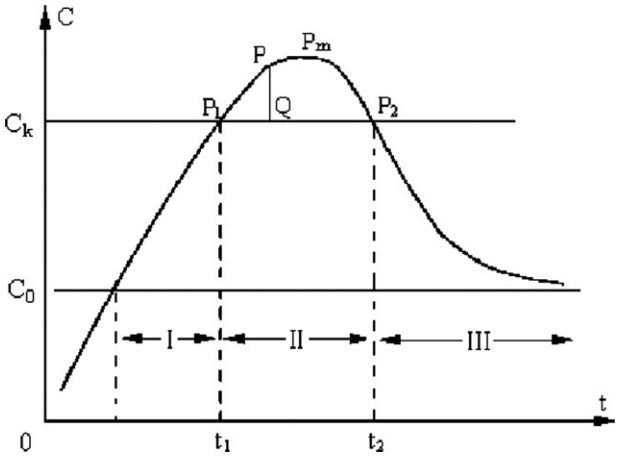

Fig. 3. Lamer graph.

Differential thermal analysis and thermal gravimetric analysis (DTA–TGA) of the dried precursor was performed on a DTA–TGA analyzer (DTA–TG, NETZSCH STA409PC, Gebruder, Germany) with Ar as the protective gas and air as the purge gas, and the heating rate is 10 K/min. The phase formation process, microstructure and crystallization of the powders were investigated by a X-ray diffractometer (XRD, 08DISCOVER, using nickel-filtered Cu-Kα radiation), field emission scanning electron microscope (SEM, HITACHI S-5500D) and JEOLJEM-2010 transmission

electron microscope (TEM, JEOLJEM-2010, Kyoto, Japan), respectively. The sintering was conducted at 1300 °C and 40 MPa for 3 min by the spark plasma sintering (SPS-1050 T, Sumitomo Coal Mining Co., Ltd). The heating rate was 100 °C/min. After sintering, the specimens were annealed at 800 °C for 20 h in air.

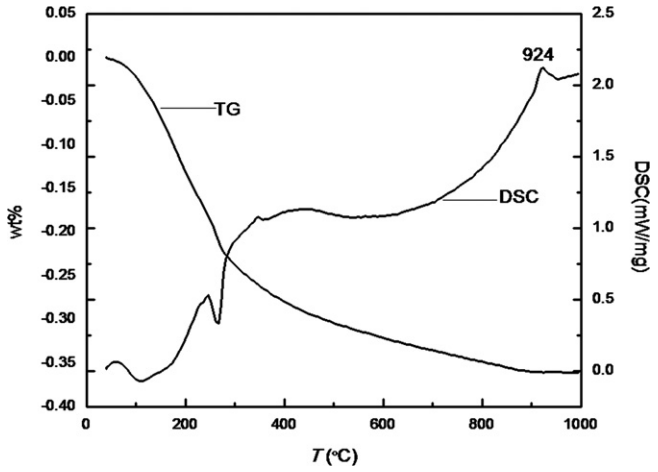

Fig. 4. Differential thermal analysis and thermal gravimetric analysis (DTA–TGA) of the precipitate precursor.

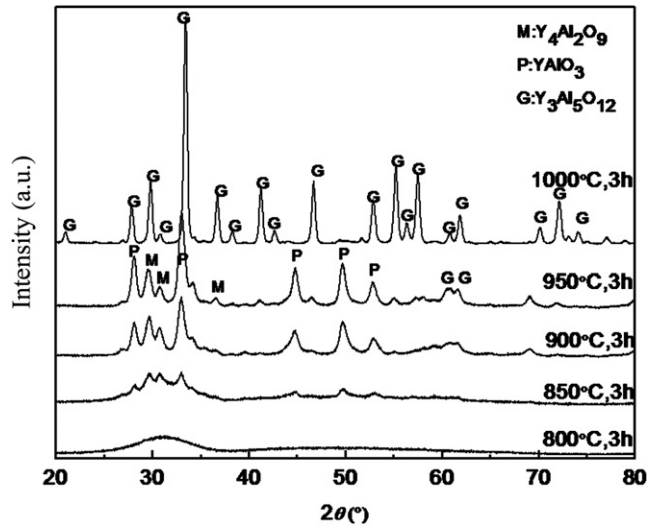

Fig. 5. XRD patterns of YAG powders from precursor ① calcined at different temperatures for 3 h.

3. Result and discussion

The mean droplet size of generated microdroplets was estimated in accordance to the following Lang's equation:

$$D_o = 0.34\left(8\pi\gamma/\rho f^2\right)^{0.33}$$

where γ is the liquid (solution) surface tension (10^{-3} Nm^{-1}), f is the ultrasound frequency (10^6 Hz), and ρ is the liquid (solution) density (10^{-3} kg m^{-3}).

Supposing $\rho = 0.99704 \times 10^{-3}$ kg m^{-3} and surface tension $\gamma = 71.97 \times 10^{-3}$ Nm^{-1} (these data are for pure water at room temperature, as data of the real mixed solution are extremely hard to achieve due to the actual conditions of our lab), the diameter of microdroplets (D_o) was about 2.48 μm.

According to rate equation of mass transfer: transfer rate = (driving force × phase contact area)/mass transfer resistance, we know that in order to promote the transfer rate we should increase the driving force and phase contact area while reducing the mass transfer resistance. Compared with phase contact area, the driving force in mass transfer, i.e. the concentration gradient is very difficult to increase.

Using the ultrasonic atomization method, microdroplets with diameter of about 2.48 μm are available. Suppose 1 mL of water makes a single spherical droplet, the surface of which is 4.84 cm^2, while the cumulative surface of multiple atomized droplets with a diameter of 2.48 μm within such a spherical droplet can reach 2.42×10^4 cm^2. So the contact area of phases has been increased dramatically. High transfer rate leads to dramatically effective collision among molecules, which leads to promoted reaction rate. Moreover, ultrasonic atomization is a process that transforms high-frequency electron oscillations into mechanical vibrations in which high energy microdroplets are created. The molecules included in the high energy microdroplets are more reactive.

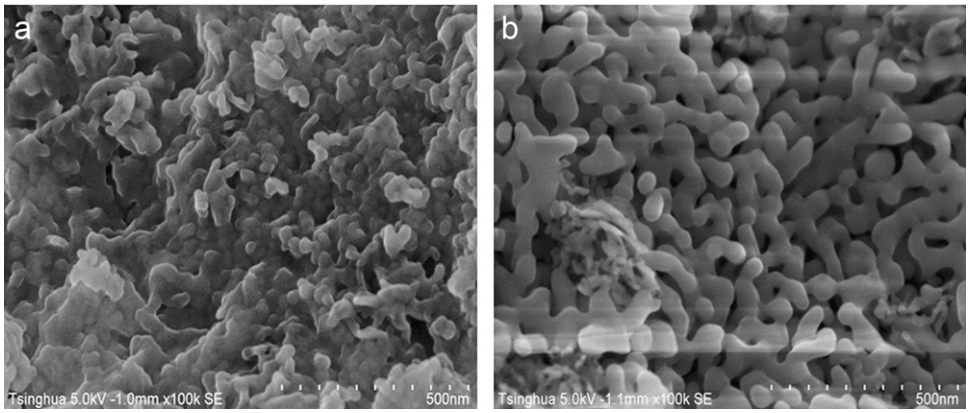

Fig. 6. Scanning electron microscope (SEM) images of the YAG powders from precursor ① calcined at (a) 900 °C and (b) 1000 °C.

From thermodynamic theory, the particle size depends on the generation rate and the growth rate of crystal nucleus, and these two kinds of rate have close relationship with the supersaturation of the solution. In order to keep the particle size uniform, a large amount of crystal nucleus should be generated simultaneously, and when the nucleus grows, no more nucleus generates.

As is shown in Lamet graph (Fig. 3): no nucleus is generated in Section 1; in Section 2, nucleus begins to take shape; and in Section 3, the nucleus grows and no new nucleus is formed. Therefore, uniform particles can be obtained with proper control of Section 2.

By means of ultrasonic atomization, we can get a great amount of nucleus. The generation of nucleus cuts down the supersaturation of the solution immediately and this conversely leads the growth rate of the nucleus to slow down. All of the above will benefit for the generation of ultrafine powders.

Thermal decomposition and crystallization temperature of the dried precursor were studied by simultaneous DTA–TGA analysis (as shown in Fig. 4, the concentration of Al^{3+} was 0.5 mol/L). The wide endothermic peak between 100 °C and 300 °C was assigned to the removal of water and alcohol. Major mass loss of the precursor took place below 300 °C, corresponding to about 25% of the total weight. The mass loss slowed down between 300 °C and 900 °C and almost completed at around 900 °C. In this period, mass loss of about 10% of the total weight was mainly caused by the decomposition of carbonate species into oxide. There was a small exothermic peak at 924 °C, which was attributed to the crystallization of YAG and YAP. This conclusion can be supported by the results of XRD (Fig. 5).

Fig. 5 shows the XRD patterns of YAG powders from precursor ① calcined at different temperatures ranging from 800 °C to 1000 °C for 3 h. No obvious diffraction peaks were observed for the sample calcined at 800 °C, indicating that the as-precipitated powders were still amorphous below this temperature, which was consistent with the DTA–TGA results (Fig. 4). After calcination at 1000 °C for 3 h, the precursor was crystallized as pure YAG.

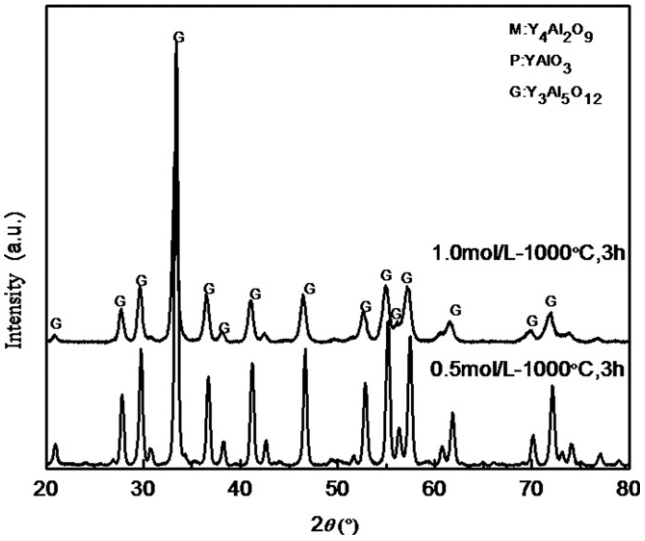

Fig. 7. XRD patterns of YAG powders from precursor ① and ② calcined at 1000 °C.

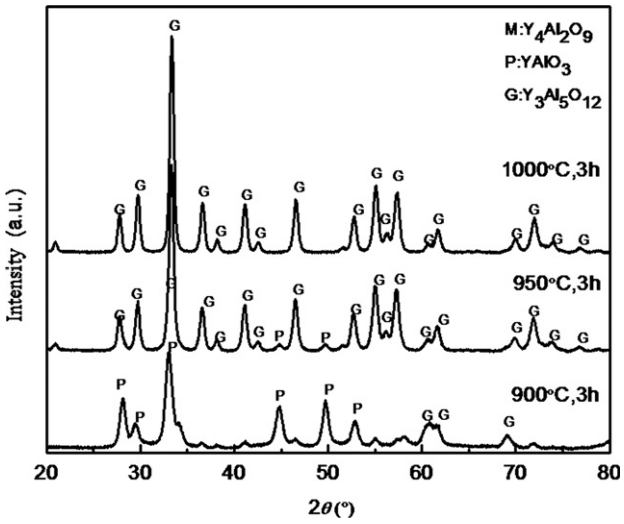

Fig. 9. XRD patterns of YAG powders from precursor ③ calcined at different temperatures.

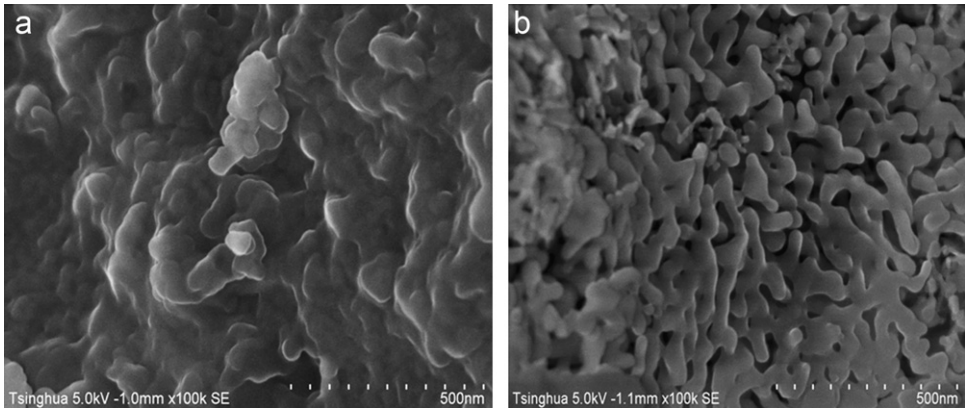

Fig. 8. Scanning electron microscope (SEM) images of the YAG powders from the precursor ② calcined at (a) 900 °C and (b) 1000 °C.

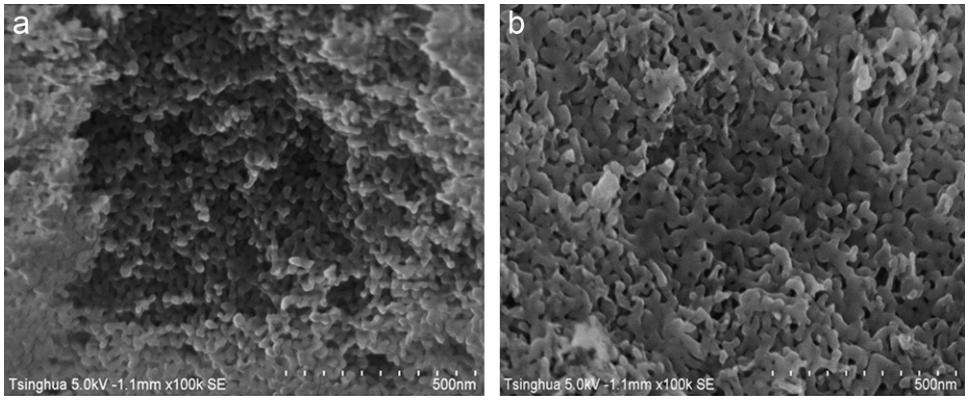

Fig. 10. Scanning electron microscope (SEM) images of the YAG powders from the precursor ③ calcined at (a) 900 °C and (b) 1000 °C.

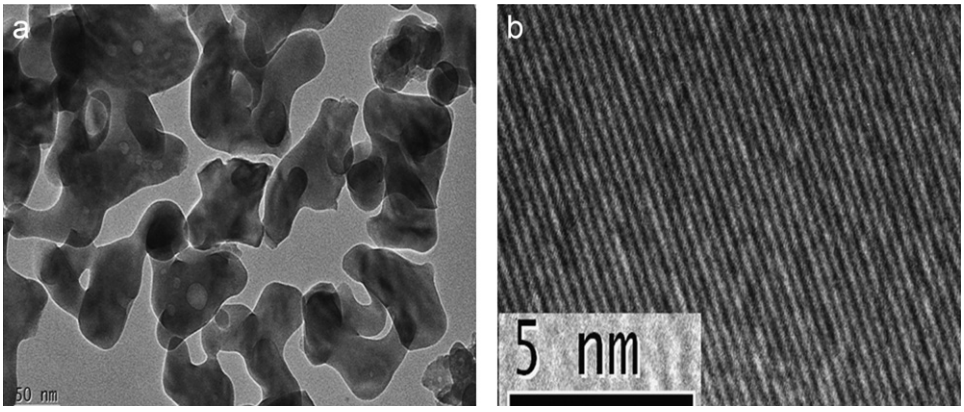

Fig. 11. (a) TEM and (b) HRTEM images of the YAG powders from precursor ③ calcined at 1000 °C for 3 h.

Fig. 6 shows the microstructure of YAG powders from precursor ① calcined at different temperatures. The average particle size of the powders calcined at 1000 °C was about 50 nm, and the particles were well dispersed.

Increasing the concentration of the mixed solution to 1 mol/L, the temperature of transforming to pure YAG did not increase correspondingly (as shown in Fig. 7). The Ultrasonic spray co-precipitation method made the higher concentration of mixed solution possible, which leads to higher efficiency. However, at the same time, the agglomeration became a little bit severer (as shown in Fig. 8).

Comparing the XRD patterns of microdroplets sprayed from the top and the side of the reactor (Fig. 9 and Fig. 5), we can easily discern that the device 2 is better than the device 1 for there was no YAM phase detected in the powders produced by device 2 below 1000 °C. This result indicated that top spray is better than side spray. The SEM photos show the microstructure of the powders, indicating the particles were well dispersed (Fig. 10).

Fig.11 shows TEM images of YAG powders from the precursor ③ calcined at 1000 °C for 3 h. Fig.11(a) clearly indicates that the powders were well dispersed, with an average grain size of 50 nm. The clear lattice fringe shown in Fig.11(b) reveals good crystallization of the powder.

Precursor ③ calcined at 1000 °C for 3 h was uniaxially pressed in a 20 mm die at 15 MPa. The sintering was conducted at 1300 °C and 40 MPa for 3 min by the spark plasma sintering (SPS). The heating rate was 100 °C/min. After sintering, the specimens were annealed at 800 °C for 20 h in air. The specimens remain gray after annealing and only the edges of the specimens appear to be translucent, which is caused by carburizing as an inevitable result of spark plasma sintering.

The density of the specimens is 4.5510 g/cm^3 measured by the Archimedes technique. The relative density is 99.95% when taking 4.5533 g/cm^3 as the theoretical density. The relative density is much higher than that mentioned in other papers (e.g. Chaima conducted sintering at 100 MPa and 1300 °C for 3 min resulting a relative density below 90%) [34]. The powders produced in this experiment are much easier to achieve high relative density which is the precondition of transparent ceramics, in other words, these powders have an obvious advantage in sintering behavior.

4. Conclusion

Homogenously dispersed nanocrystalline YAG powders were synthesized via ultrasonic spray co-precipitation with ammonia as precipitation agent. DTA–TGA and XRD results indicate that the as-synthesized precursor could be converted to pure YAG phase after being calcined at

1000 °C for 3 h. Compared with the side spray, the top spray is better, for there is no YAM phase detected in the powders below 1000 °C. SEM results reveal that the particles, sizes of which are about 50 nm, are well dispersed. TEM results that show the clear lattice fringe reveal a good crystallization of the powder. Increasing the concentration of the mixed solution, the temperature of transforming to pure YAG did not increase correspondingly which shows the potential competence in high yield efficiency which is always a problem with other methods. After sintering at 1300 °C and 40 MPa for 3 min by the SPS, we got ceramics with high relative density of 99.95% which is much higher than Chaima's 90%. After annealing, the edge of the specimen appears to be translucent. Considering the inevitable carburizing by using the spark plasma sintering, these powders are anticipated to be used as candidates for sintering transparent ceramic materials if we conduct the sintering with a vacuum furnace.

References

[1] T. Yokoyama, Single crystal for solid-state laser material, Bulletin of the Ceramic Society of Japan 23 (1988) 461–463.

[2] S. Masami, H. Hajime, S. Shirasaki, et al., Optical spectra of undoped and rare-earth (=Pr, Nd, Eu, and Er) doped transparent ceramics $Y_3Al_5O_{12}$, Journal of Applied Physics 69 (1991) 3709–3718.

[3] A. Ikesue, I. Furusato, K. Kamata, Fabrication of polycrystalline transparent YAG ceramics by a solid-state reaction method, Journal of the American Ceramic Society 78 (1) (1995) 225–228.

[4] A.R. Nagham, J.Y. Lee, Preparation of spinel lithium manganese oxide by aqueous co-precipitation, Journal of Power Sources 85 (2000) 284–293.

[5] V.B. Glushkova, V.A. Krzhizhanovskaya, O.N. Egorova, Mechanism of YAG synthesized by the solid-state reaction method, Journal of Inorganic Materials 19 (1983) 80–84.

[6] S.H. Lee, S. Kochawattana, G.L. Messing, et al., Solid-state reactive sintering of transparent polycrystalline Nd:YAG ceramic, Journal of the American Ceramic Society 89 (6) (2006) 1945–1950.

[7] X.D. Li, J.G. Li, Z.M. Xiu, et al., Transparent Nd:YAG ceramics fabricated using nanosized γ-alumina and yttria powders, Journal of the American Ceramic Society 92 (1) (2009) 241–244.

[8] A. Maitre, C. Salle, R. Boulesteix, et al., Effect of silica on the reactive sintering of polycrystalline Nd:YAG ceramic, Journal of the American Ceramic Society 91 (2) (2008) 406–413.

[9] I. Sakaguchi, H. Haneda, J. Tanaka, Effect of composition on the oxygen tracer diffusion in transparent yttrium aluminum garnet (YAG) ceramics, Journal of the American Ceramic Society 79 (6) (1996) 1627–1632.

[10] Y.S. Wu, J. Li, Y.B. Pan, et al., Diode-pumped Yb:YAG ceramic laser, Journal of the American Ceramic Society 90 (10) (2007) 3334–3337.

[11] S.H. Lee, E.R. Kupp, A.J. Stevenson, et al., Hot isostatic pressing of transparent Nd:YAG ceramics, Journal of the American Ceramic Society 92 (7) (2009) 1456–1463.

[12] S.H. Tong, T.C. Lu, W. Guo, Synthesis of YAG powder by alcohol-water co-precipitation method, Journal of Materials Letters 61 (2007) 4278–4289.

[13] H. Gong, D.Y. Tang, H. Huang, Agglomeration control of Nd:YAG nanoparticles via freeze drying for transparent Nd:YAG ceramics, Journal of the American Ceramic Society 92 (4) (2009) 812–817.

[14] M. Suarez, A. Fernandez, J.L. Menendez, et al., Hot isostatic pressing of optically active Nd: YAG powders doped by a colloidal processing route, Journal of the European Ceramic Society 30 (2010) 1489–1494.

[15] P. Sellappan, V. Jayaram, A.H. Chokshi, Synthesis of bulk, dense, nanocrystalline yttrium aluminum garnet from amorphous powders, Journal of the American Ceramic Society 90 (11) (2007) 3638–3641.

[16] G.G. Xu, X.D. Zhang, W. He, et al., The study of surfactant application on synthesis of YAG nano-sized powders, Journal of Powder Technology 163 (2006) 202–205.

[17] Z.H. Chen, Y. Yang, Z.G. Hu, et al., Synthesis of highly sinterable YAG nanopowders by a modified co-precipitation method, Journal of Alloys and Compounds 433 (2007) 328–331.

[18] X.X. Li, W.J. Wang, Nanosturctured yttrium aluminum garnet powders synthesized by co-precipitation method using tetraethylene-pentamine, Journal of Rare Earths 27 (6) (2009) 967–970.

[19] X.X. Li, W.J. Wang, Preparation of uniformly dispersed YAG ultrafine powders by co-precipitation method with SDS treatment, Journal of Powder Technology 196 (2009) 26–29.

[20] Y.T. Nien, Photoluminescence enhancement of $Y_3Al_5O_{12}$:Ce nanoparticles using HMDS, Journal of the American Ceramic Society 91 (11) (2008) 3599–3602.

[21] Y.T. Nien, Improved photoluminescence of $Y_3Al_5O_{12}$:Ce nanoparticles by silica coating, Journal of the American Ceramic Society 93 (6) (2010) 1688–1691.

[22] Y. Ru, Q. Jie, L. Min, et al., Synthesis of yttrium aluminum garnet (YAG) powder by homogeneous precipitation combined with supercritical carbon dioxide or ethanol fluid drying, Journal of the European Ceramic Society 28 (2008) 2903–2914.

[23] J.Q. Wang, S.H. Zheng, Microwave synthesis of homogeneous YAG nanopowder leading to a transparent ceramic, Journal of the American Ceramic Society 92 (6) (2009) 1217–1223.

[24] B. Hoghooghi, L. Healey, S. Powell, et al., Synthesis of YAG:Cr phosphors by precipitation from aluminum and yttrium sulfate solution, Materials Chemistry and Physics 38 (2) (1994) 175–180.

[25] D.J. Sordelet, M. Akinc, M.L. Panchula, et al., Synthesis of yttrium aluminum garnet precursor powders by homogeneous precipitation, Journal of the European Ceramic Society 14 (2) (1994) 123–130.

[26] J. Li, Y.B. Pan, F.G. Qiu, et al., Synthesis of nanosized Nd:YAG powders via gel combustion, Ceramics International 33 (2007) 1047–1052.

[27] J. Li, Y.B. Pan, F.G. Qiu, et al., Nanostuctured Nd:YAG powders via gel combustion: the influence of citrate-to-nitrate ratio, Ceramics International 34 (2008) 141–149.

[28] M. Veith, S. Mathur, A. Kareiva, et al., Low temperature synthesis of nanocrystalline $Y_3Al_5O_{12}$ (YAG) and Ce-doped $Y_3Al_5O_{12}$ via different Sol–gel methods, Journal Of Materials Chemistry 9 (12) (1999) 3069–3079.

[29] H.M. Wang, M.C. Simmonds, Synthesis of nanosize powders and thin films of Yb-doped YAG by Sol–gel methods, Journal of Materials Chemistry 15 (2003) 3474–3480.

[30] Y.Q. Liu, L. Gao, Low-temperature synthesis of nanocrystalline yttrium aluminum garnet powder using triethanolamine, Journal of the American Ceramic Society 86 (10) (2003) 1651–1653.

[31] X.D. Zhang, H. Liu, W. He, J.Y. Wang, X. Li, R.I. Boughton, Novel synthesis of YAG by solvothermal method, Journal of Crystal Growth 275 (2005) 1913–1917.

[32] Y.G. Wang, L.G. Zhang, Y. Fan, et al., Synthesis, characterization, and optical properties of pristine and doped yttrium aluminum garnet nanopowders, Journal of the American Ceramic Society 88 (2) (2005) 284–286.

[33] Y.C. Kang, I.W. Lenggoro, S.B. Park, et al., YAG:Ce phosphor particles prepared by ultrasonic spray pyrolysis, Materials Research Bulletin 35 (2000) 789–798.

[34] R. Chaima, R. Marder-Jaeckel, J.Z. Shen, Transparent YAG ceramics by surface softening of nanoparticles in spark plasma sintering, Materials Science and Engineering A 429 (2006) 74–78.